BIOCHEMISTRY
including biophysical chemistry & molecular biology

Article

pubs.acs.org/biochemistry

Intermonomer Electron Transfer between the *b* Hemes of Heterodimeric Cytochrome bc_1

Pascal Lanciano, Bahia Khalfaoui-Hassani, Nur Selamoglu, and Fevzi Daldal*

Department of Biology, University of Pennsylvania, Philadelphia, Pennsylvania 19104, United States

Supporting Information

ABSTRACT: The ubihydroquinone:cytochrome *c* oxidoreductase, or cytochrome bc_1, is a central component of respiratory and photosynthetic energy transduction pathways in many organisms. It contributes to the generation of membrane potential and proton gradient used for cellular energy (ATP) production. The three-dimensional structures of cytochrome bc_1 show a homodimeric organization of its three catalytic subunits. The unusual architecture revived the issue of whether the monomers operate independently or function cooperatively during the catalytic cycle of the enzyme. In recent years, different genetic approaches allowed the successful production of heterodimeric cytochrome bc_1 variants and evidenced the occurrence of intermonomer electron transfer between the monomers of this enzyme. Here we used a version of the "two-plasmid" genetic system, also described in the preceding paper (DOI: 10.1021/bi400560p), to study a new heterodimeric mutant variant of cytochrome bc_1. The strain producing this heterodimeric variant sustained photosynthetic growth of *Rhodobacter capsulatus* and yielded an active heterodimer. Interestingly, kinetic data showed equilibration of electrons among the four *b* heme cofactors of the heterodimer, via "reverse" intermonomer electron transfer between the b_L hemes. Both inactive homodimeric and active heterodimeric cytochrome bc_1 variants were purified to homogeneity from the same cells, and purified samples were subjected to mass spectrometry analyses. The data unequivocally supported the idea that the cytochrome *b* subunits carried the expected mutations and their associated epitope tags. Implications of these findings on our interpretation of light-activated transient cytochrome *b* and *c* redox kinetics and the mechanism of function of a dimeric cytochrome bc_1 are discussed with respect to the previously proposed heterodimeric Q cycle model.

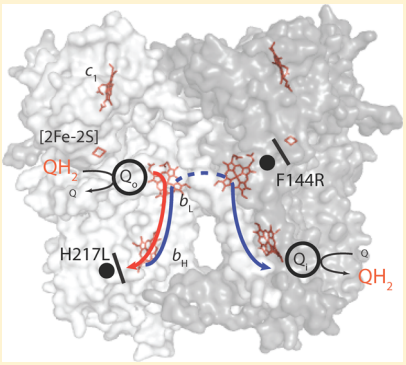

The ubihydroquinone:cytochrome *c* oxidoreductase (also called cytochrome bc_1 or complex III) is a multisubunit membrane-bound enzyme that is central to respiratory and photosynthetic energy transduction pathways in various organisms.[1] It converts hydroquinones (QH_2) to quinones (Q), reduces various electron carriers (often cytochromes *c*), and contributes to the formation of the membrane potential and proton gradient that are used for cellular ATP production.[2,3] In most bacteria, like *Rhodobacter capsulatus*, cytochrome bc_1 consists of three universally conserved catalytic subunits: the Fe−S protein, cytochrome *b*, and cytochrome c_1.[4,5] Cytochrome *b* is an integral membrane protein, whereas the Fe−S protein and cytochrome c_1 are membrane-anchored by their amino- and carboxyl-terminal helices, respectively. These subunits carry specific cofactors that are essential for enzyme activity. The cofactors are the high-redox midpoint potential (E_m) [2Fe-2S] cluster in the Fe−S protein, the two *b*-type hemes with one low-E_m (b_L) and one high-E_m (b_H) heme in cytochrome *b*, and the high-E_m *c*-type heme in cytochrome c_1.[6] Available three-dimensional structures of cytochrome bc_1 from various organisms depict this enzyme as a symmetrical homodimer with each Fe−S protein spanning both monomers.[7−9] In addition, the dimer interface between cytochrome *b* subunits brings the low-E_m b_L hemes of the two monomers very close to each other (~11 Å). These observations led to the intriguing possibility of intermonomer electron equilibration between the *b* hemes of cytochrome *b* subunits in dimeric cytochrome bc_1.

The modified Q cycle used to describe the cytochrome bc_1 mechanism of function requires two consecutive Q_o site-mediated QH_2 oxidations for a complete catalytic cycle.[10] Whether the two consecutive QH_2 oxidations occur only in a given monomer as initially described[11] or whether they alternate between the two Q_o sites of a dimeric enzyme is unknown. Over the years, several groups, including our own, provided experimental data that could be interpreted in different ways,[12−15] especially in light of the symmetrical homodimeric cytochrome bc_1 structures. Because of the inherent symmetry, the intramonomer versus intermonomer electron transfers between the *b* heme cofactors of cytochrome bc_1 cannot be readily discerned from each other.[16] However, recent genetic approaches successfully produced asymmetric monomers to yield heterodimeric cytochrome bc_1 variants and provided data supporting intermonomer electron transfer.[17−19]

Previously, we developed a two-plasmid genetic system to produce heterodimeric cytochrome bc_1 variants.[19,20] The system used two independently expressed *petABC* operons

Received: May 2, 2013
Revised: September 10, 2013
Published: September 12, 2013

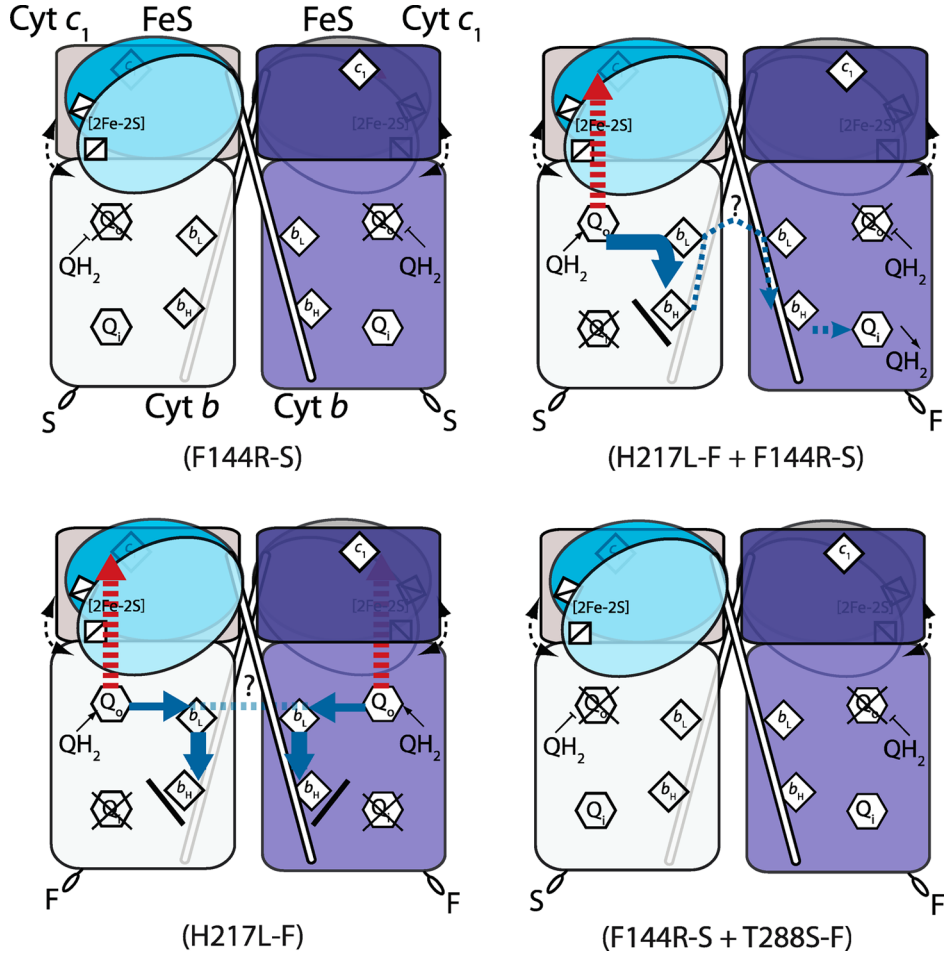

Figure 1. *R. capsulatus* system for studying intra- and intermonomer electron transfer in dimeric cytochrome bc_1. Coexpression of a Kan^R plasmid carrying *petABC* with the cyt *b*-S F144R mutation and a Tet^R plasmid carrying *petABC* with the cyt *b*-F H217L mutation yields inactive homodimeric cyt *b*-S F144R (top left) and cyt *b*-F H217L (bottom left) as well as active heterodimeric (cyt *b*-F H217L + cyt *b*-S F144R) (top right) cytochrome bc_1 variants. An inactive heterodimer with two inactive Q_o sites (cyt *b*-S F144R + cyt *b*-F T288S) used as a control is also shown (bottom right). Thick red dashed and thick blue solid arrows correspond to electron transfer to the high- and low-potential cofactor chains of cytochrome bc_1, respectively. Inactive Q_o or Q_i sites are indicated by X's, and the thin dotted line depicts the proposed reverse electron transfer between the hemes b_L and electron equilibration among all *b* hemes of the active heterodimeric cytochrome bc_1.

carried by two plasmids of different replicons, coharbored by a cell lacking its endogenous cytochrome bc_1. Each plasmid carried a differently mutated and epitope-tagged cytochrome *b* and produced homodimeric and heterodimeric variants in the same cell. By selective inactivation of the Q_o site of one monomer and the Q_i site of the other monomer, evidence was obtained for the occurrence of intermonomer electron transfer between the b_L hemes of cytochrome bc_1.[19] In this case, QH_2 oxidation at the Q_o site was restricted using the cyt *b* Y147A mutation, which abolishes reduction of the low-potential chain (hemes b_L and b_H) of the enzyme.[21] Similarly, the Q_i site was also disabled by the cyt *b* H212N mutation, which causes loss of heme b_H.[22] Strains that produced only a homodimeric mutant cytochrome bc_1 were unable to grow photosynthetically (Ps^-) as they produced inactive homodimers. In contrast, cells producing both homodimeric and heterodimeric cytochrome bc_1 variants exhibited slow Ps growth ($Ps^{+/-}$) compared to that of a wild-type strain and contained partially active cytochrome bc_1 equated with the heterodimeric variants.[19] Time-resolved, light-activated single-turnover kinetics showed that intermolecular b_L-b_L-b_H heme electron transfer occurred in membranes from these cells at a rate slower (in the presence of the Q_i site inhibitor antimycin) than the rate of intramonomer b_L-b_H heme electron transfer seen in a wild-type enzyme under similar conditions.[19] We also observed that strains carrying the two-plasmid system formed rare ($\sim 10^{-4}$) large Ps^+ colonies among a population of predominantly small $Ps^{+/-}$ colonies.[19,20]

In our ongoing work, we characterized extensively both genetic and biochemical properties of the two-plasmid system that produces heterodimeric cytochrome bc_1. First, in the preceding paper (DOI: 10.1021/bi400560p), we addressed the molecular basis of the genetic rearrangements that occur when two identical plasmids (i.e., the same replicon) are used. We found that the large Ps^+ colonies contained co-integrant plasmids predominantly formed via RecA-mediated recombination between the initial plasmids, and yielded increased amounts of active heterodimers, and better Ps growth [preceding paper (DOI: 10.1021/bi400560p)]. The co-integrant plasmids faithfully carried both the initial cytochrome *b* mutations and their associated epitope tags and reliably produced heterodimeric cytochrome bc_1 variants [preceding paper (DOI: 10.1021/bi400560p)]. Second, using this improved system with a set of Q_o and Q_i site mutations different from those used previously,[19] we produced a novel

dx.doi.org/10.1021/bi400561e | *Biochemistry* 2013, 52, 7196−7206

heterodimeric cytochrome bc_1 (Figure 1) that supported efficient Ps^+ growth and exhibited intermonomer reverse electron transfer among all four *b* hemes of cytochrome bc_1. This strain allowed large-scale purification of inactive homodimeric and active heterodimeric variants from the same cells. Analysis of purified proteins by mass spectrometry showed that they carried the expected cytochrome *b* mutations and their associated epitope tags. We conclude that the two-plasmid system produces reliably heterodimeric cytochrome bc_1 variants that support Ps (cytochrome bc_1-dependent) growth. Available data indicate that intermonomer reverse electron transfer occurs among the b_H, b_L, b_L, and b_H hemes of a dimeric enzyme, consistent with the heterodimeric Q cycle model.[15] These findings are discussed in terms of light-activated transient cytochrome *b* and *c* redox kinetics and in the context of the mechanism of function of cytochrome bc_1.

MATERIALS AND METHODS

Bacterial Strains and Growth Conditions. All *R. capsulatus* strains harboring the plasmids that express the cytochrome bc_1 mutants were derivatives of strain MT-RBC1 [Δ(*petABC::spe*)] or BK-RBC1 [Δ(*petABC::spe*) Δ(*recA*)] [preceding paper (DOI: 10.1021/bi400560p)] carrying a complete chromosomal deletion of *petABC* in a $RecA^+$ or $RecA^-$ background, respectively. They were grown in liquid or solid enriched (MPYE) medium, supplemented with antibiotics as appropriate [10 μg/mL kanamycin (Kan), 2.5 μg/mL tetracycline (Tet) and 10 μg/mL spectinomycin] under either Res (semiaerobic and dark) or Ps (photoheterotrophic and light) conditions at 35 °C, as described previously.[23] For Res growth, 1 L cultures in 2 L flasks were used. Plates were placed either in a dark incubator (Res) or in anaerobic jars with gas packs generating H_2 and CO_2 (Becton Dickinson Inc.) in temperature-controlled Percival light incubators (Ps).

Escherichia coli strains harboring the plasmids used were derived from HB101 [F^- Δ(*gpt-proA*)*62 araC14 leuB6*(Am) *glnV44*(AS) *galK2*(Oc) *lacY1* Δ(*mcrC-mrr*) *rpsL20*(Str^r) *xylA5 mtl-1 thi-1*] and grown on Luria-Bertani medium containing ampicillin, Kan, or Tet (100, 50, or 12.5 μg/mL, respectively) as appropriate.[4] *R. capsulatus* strains coharboring two plasmids with the same type (*inc*Q/P4) of replicon were obtained via triparental matings as described previously[5] and as in the preceding paper (DOI: 10.1021/bi400560p). Strains coharboring two plasmids were maintained using half amounts of Kan and Tet, normally used for selection, and as a precautionary measure, large cultures were subjected to short periods of growth (~24 h) as described previously.[19] Under these conditions, large Ps^+ colonies were observed at frequencies of $\lesssim 10^{-4}$ in the $RecA^+$ and $RecA^-$ backgrounds with strains harboring two plasmids. Cultures that occasionally yielded more than ~0.01% large Ps^+ clones were discarded.

Molecular Genetic and Biochemical Techniques. Molecular genetic techniques were performed using standard procedures,[24] as described in detail in the preceding paper (DOI: 10.1021/bi400560p). Intracytoplasmic (chromatophore) membranes were obtained from frozen washed cells after two passages through a French press, as described previously.[25] Protein concentrations were determined using the bicinchoninic acid method[26] with bovine serum albumin as a standard. Sodium dodecyl sulfate−polyacrylamide gel electrophoresis (SDS−PAGE) (12.5%) was conducted as described in ref 27, and prior to being loaded, samples were solubilized by incubation for 10 min at room temperature in 62.5 mM Tris-HCl (pH 6.8), 2% SDS, 0.1 M dithiothreitol, 25% glycerol, and 0.01% bromophenol blue. Immunoblot analyses were conducted as described in ref 19 using polyclonal antibodies against *R. capsulatus* cytochrome *b* or monoclonal anti-Flag (Sigma Inc.) and anti-Strep (Novagen Inc.) antibodies. Steady-state cytochrome bc_1 activity was measured using decylbenzohydroquinone (DBH_2) as an electron donor and horse heart cytochrome *c* as an electron acceptor at 25 °C.[5] The reaction was initiated by enzyme addition and monitored at 550 nm for 1 min, and the portion of the initial rate that was famoxadone sensitive was taken as the enzyme activity. *R. capsulatus* cytochrome bc_1 was purified and stored at −80 °C as described in ref 19.

Spectroscopic Techniques. Optical spectra were recorded on a Cary 60 spectrophotometer (Agilent Technologies Inc.). Absorption difference spectra for the *c*- and *b*-type cytochromes were obtained using chromatophore membranes (0.3 mg of total protein/mL), oxidized with potassium ferricyanide, and reduced with sodium ascorbate or sodium dithionite, as appropriate. EPR measurements were performed on a Bruker Elexsys E500 spectrometer. X-Band EPR spectra were recorded using a standard Bruker cavity (ER 4102ST) fitted to a helium flow cryostat (ESR900, Oxford Instruments). Spectrometer settings are indicated in figure legends.

Time-resolved, light-activated kinetic spectroscopy was performed on a dual-wavelength kinetic spectrophotometer with chromatophore membranes resuspended in 50 mM MOPS (pH 7.0) and 100 mM KCl buffer supplemented with 100 μM ferricyanide (FeCN, 430 mV), 8 μM DAD (260 mV), 6 μM NQ (145 mV), 1 μM PMS (80 mV), 1 μM PES (50 mV), 6 μM 2HNQ (−145 mV), and 6 μM benzyl viologen (BV, −359 mV) as redox mediators and 2.5 μM valinomycin as a membrane potential uncoupler.[28] The amounts of chromatophore membranes used in each assay were normalized to their reaction center (RC) content, as determined by measuring the flash-induced optical absorbance difference at 605−540 nm (E_h = 380 mV), and an extinction coefficient of 29.8 mM^{-1} cm^{-1}. Transient cytochrome *c* re-reduction and cytochrome *b* reduction kinetics at an E_h of 100 mV, initiated by a short saturating flash (~8 μs) from a xenon lamp, were followed at 550−540 and 560−570 nm, respectively. Antimycin, myxothiazol, and famoxadone were used at 10 μM each, as needed.

Mass Spectrometry. Purified cytochrome bc_1 samples were subjected to in-solution digestion with chymotrypsin (Thermo Scientific Inc.) according to the manufacturer's recommendation. Repeat sample digestions were performed in the presence of methanol to facilitate cleavage of hydrophobic portions of cytochrome *b*, and as needed, cyanogen bromide (Sigma-Aldrich Inc.) cleavage was included to target the F144 position containing peptides according to the procedure described in refs 29 and 30. Digested samples were cleaned using ZipTip (Millipore Inc.), dried and resuspended in 5 μL of 5% acetonitrile in 0.1% formic acid (buffer A), and analyzed with a nanospray LC-MS/MS Thermo LCQ Deca XP+ ion trap mass spectrometer coupled to a Thermo-Dionex LC Packings Ultimate Nano HPLC system controlled by Thermo Xcalibur version 2.0. A C18 nanocolumn (Thermo-Dionex, NAN-75-15-03-PM) was used to fractionate peptides, using a 90 min elution gradient (5 to 75% acetonitrile in 0.1% formic acid). The top three precursor ions were trapped and fragmented using dynamic exclusion to maximize the detection of unique peptides. Collected spectra were analyzed against the *R. capsulatus* protein database using Sequest and Thermo

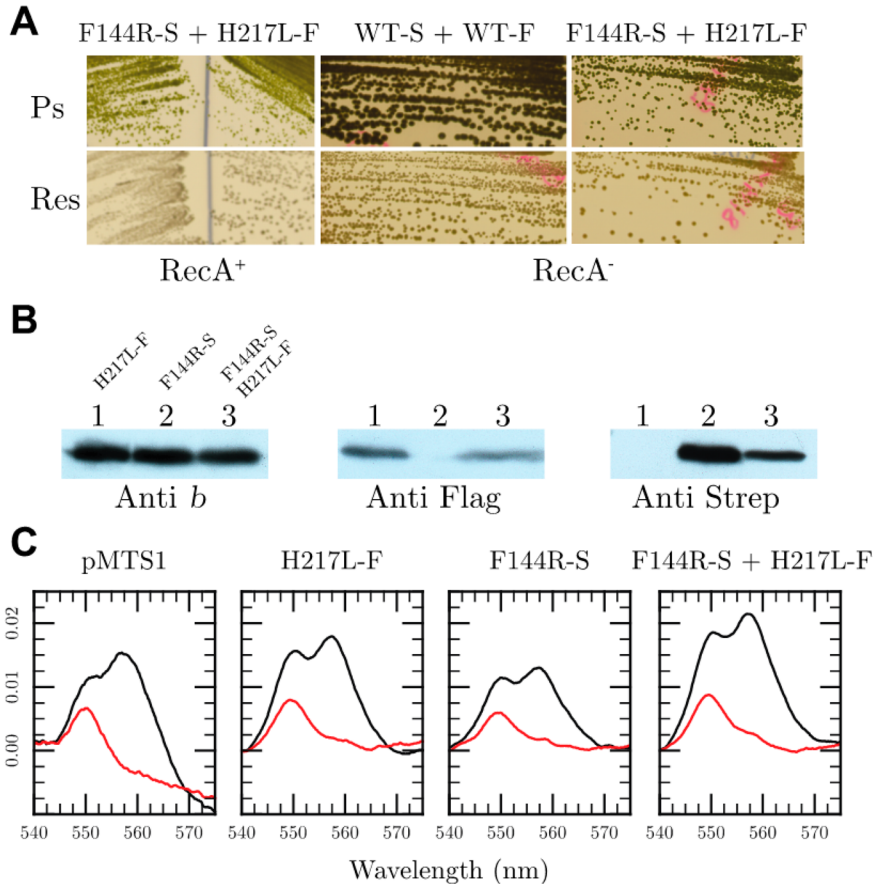

Figure 2. Growth phenotypes and biochemical properties of *R. capsulatus* strains producing heterodimeric cytochrome bc_1 variants. (A) Photosynthetic (Ps) and respiratory (Res) growth on enriched medium of *R. capsulatus* RecA$^+$ (MT-RBC1) and RecA$^-$ (BK-RBC1) strains harboring the two-plasmid system producing a heterodimeric (cyt *b*-S F144R + cyt *b*-F H217L) cytochrome bc_1 variant. (B) SDS−PAGE and immunoblot analyses of Strep- and Flag-tagged cytochrome *b* subunits in chromatophore membranes of strains harboring different combinations of Kan^R and Tet^R plasmids producing homodimeric and heterodimeric cytochrome bc_1 variants. Approximately 10 μg of total membrane proteins was used, and cytochrome *b* contents were determined using polyclonal antibodies specific to *R. capsulatus* cytochrome *b* as well as commercially available monoclonal antibodies against the Strep (S) and Flag (F) epitope tags. (C) Optical redox difference spectra to reveal total *b*-type (dithionite-reduced minus ferricyanide-oxidized) (black) and *c*-type (ascorbate-reduced minus ferricyanide-oxidized) (red) cytochrome contents of chromatophore membranes (0.3 mg/mL) obtained from appropriate *R. capsulatus* strains grown by respiration in enriched medium.

Bioworks version 3.3 with appropriate protease cleavage rules (F, W, Y, and L for chymotrypsin; M for CNBr) in full- and half-digestion modes, as needed. The computed results were filtered using standard values for X_{corr} ($\geq$1.5, 2.0, and 2.5 for *m*/*z* +1, +2, and +3, respectively) and ΔC_N ($\geq$0.1), and all significant spectra were inspected manually to validate automatic assignments.

Chemicals. The cytochrome bc_1 inhibitors antimycin A and myxothiazol were purchased from Sigma-Aldrich, and famoxadone was obtained from DuPont Inc. Dodecyl maltoside was purchased from Anatrace Inc., and decylbenzoquinone (DBH) was from Sigma-Aldrich. DEAE-BioGel A was obtained from Bio-Rad.

RESULTS

A New Heterodimeric Cytochrome bc_1 for Probing Intermonomer Electron Transfer between Its *b* Hemes. In this study, we produced a new heterodimeric cytochrome bc_1 using the improved [preceding paper (DOI: 10.1021/bi400560p)] two-plasmid genetic system. The previously produced heterodimeric cytochrome bc_1 (cyt *b*-S Y147A + cyt *b*-F H212N) could not be purified in an active form, because of its inherent instability induced by the absence of b_H heme. We thought a structurally less "perturbed" cytochrome bc_1 variant with intact cofactors would be more informative. Thus, the cyt *b* F144R[31] and cyt *b* H217L[32] mutations to inactivate the Q_o site in one monomer and the Q_i site in the other monomer, respectively, were chosen. The cyt *b* F144R mutation abolishes the transfer of an electron from QH_2 to heme b_L without affecting Q/QH_2 occupancy of the Q_o site. This Q_o site mutation is thought to form an ion pair with Q_r conferring a unique EPR signature.[31] The cyt *b* H217 residue is a highly conserved residue located in the vicinity of heme b_H and is involved in the stabilization of SQ at the Q_i site. Its substitution with leucine abolishes Q_i site catalytic activity without affecting enzyme assembly and stability.[32] As before, the cytochrome *b* subunits were tagged with Strep and Flag epitopes to produce three different populations of cytochrome bc_1 variants in a given cell.[19] These are the Q_o (cyt *b*-S F144R + cyt *b*-S F144R) and Q_i (cyt *b*-F H217L + cyt *b*-F H217L) site defective homodimers and the one-Q_o site and one-Q_i site defective heterodimer (cyt *b*-S F144R + cyt *b*-F H217L) (Figure 1).

Growth Properties of *R. capsulatus* Strains Producing Homodimeric and Heterodimeric Cytochrome bc_1 Variants. *R. capsulatus* strains harboring a single plasmid

dx.doi.org/10.1021/bi400561e | *Biochemistry* 2013, 52, 7196−7206

with wild-type *petABC* (pMTS1-S carrying a Strep epitope-tagged or pMTS1-F carrying a Flag epitope-tagged cytochrome *b*) were Ps^+ and produced active homodimeric cytochrome bc_1, whereas those with a single cytochrome *b* mutation (cyt *b*-S F144R or cyt *b*-F H217L) were Ps^- (not shown) and produced inactive, homodimeric cytochrome bc_1 [ref 19 and the preceding paper (DOI: 10.1021/bi400560p)]. The control strains harboring a two-plasmid system with epitope-tagged wild-type copies of *petABC* (cyt *b*-S + cyt *b*-F) were Ps^+, and those carrying a two-plasmid system with two Q_o site mutations (cyt *b*-S F144R + cyt *b*-F T288S) were Ps^- (data not shown) (the cyt *b* T288S mutation that inactivates the Q_o site was reported previously[33]) (Figure 1) [preceding paper (DOI: 10.1021/bi400560p)]. Unlike the controls, both the $RecA^+$ (MT-RBC1) and $RecA^-$ (BK-RBC1) cells harboring the two-plasmid system with (cyt *b*-S F144R + cyt *b*-F H217L) mutations exhibited Ps^+ growth (Figure 2A). As described in the preceding paper (DOI: 10.1021/bi400560p), the $RecA^-$ strains grew slower under both Ps and Res conditions than the $RecA^+$ strains. Cells carrying the two-plasmid system with (cyt *b*-S F144R + cyt *b*-F H217L) formed smaller $Ps^{+/-}$ colonies than their corresponding wild-type parents. They exhibited rare large Ps^+ colonies at frequencies of $\lesssim 10^{-4}$ in $RecA^+$ and $RecA^-$ backgrounds, and these colonies contained co-integrant plasmids that conserved faithfully the cyt *b* mutations and their associated epitope tags [preceding paper (DOI: 10.1021/bi400560p)]. This process is still not understood completely and deserves further study.

Biochemical Properties of *R. capsulatus* Strains Producing Homodimeric and Heterodimeric Cytochrome bc_1 Variants. SDS−PAGE and immunoblot analyses of appropriate strains using antibodies against cytochrome *b* or Strep or Flag epitopes indicated that cells harboring two plasmids exhibited both Strep- and Flag-tagged cytochrome bc_1 variants, similar to the corresponding single-epitope-tagged wild-type strains (Figure 2B). As the different epitope tag antibodies exhibit different affinities for their antigens, a better comparison of the amounts of cytochrome bc_1 produced in these strains was provided by optical spectroscopy. Chromatophore membranes of appropriate cells carrying the different plasmids showed that the optical spectra in the α region for the reduced cytochrome *b* at 560 nm and the high-potential cytochromes *c* at 550 nm were comparable to those of a wild-type parent (pMTS1) (Figure 2C). Thus, the mutation selected to inactivate the Q_o and Q_i sites did not alter the biogenesis of cytochrome bc_1 and its cofactors to produce the expected homodimeric and heterodimeric variants.

Next, the cofactors of cytochrome bc_1 were examined by EPR spectroscopy (Figure 3). The EPR resonance lines at 3.78 and 3.43, corresponding to the g_z feature of oxidized b_L and b_H hemes, respectively, were detected in membranes of cells producing cyt *b*-S F144R + cyt *b*-F H217L homodimers as well as cells producing the heterodimeric variant (cyt *b*-S F144R + cyt *b*-F H217L) (Figure 3A). Although the amplitudes and shapes of the resonance lines were similar to those seen with a wild-type strain, the g_z values were different for the cyt *b*-S F144R and cyt *b*-F H217L variants. Chromatophore membranes containing the homodimeric cyt *b*-S F144R exhibited a wild-type-like cytochrome b_H g_z value centered at 3.43, whereas those of cyt *b*-F H217L had a g_z value centered at 3.49 (Figure 3A), probably caused by the local modifications of the heme b_H environment in this Q_i site mutation. Interestingly, chromatophore membranes of the strain carrying the (cyt *b*-S F144R + cyt *b*-F H217L) combination exhibited an intermediate g_z value at 3.46 (Figure 3A). The EPR spectra of cytochrome bc_1 [2Fe-

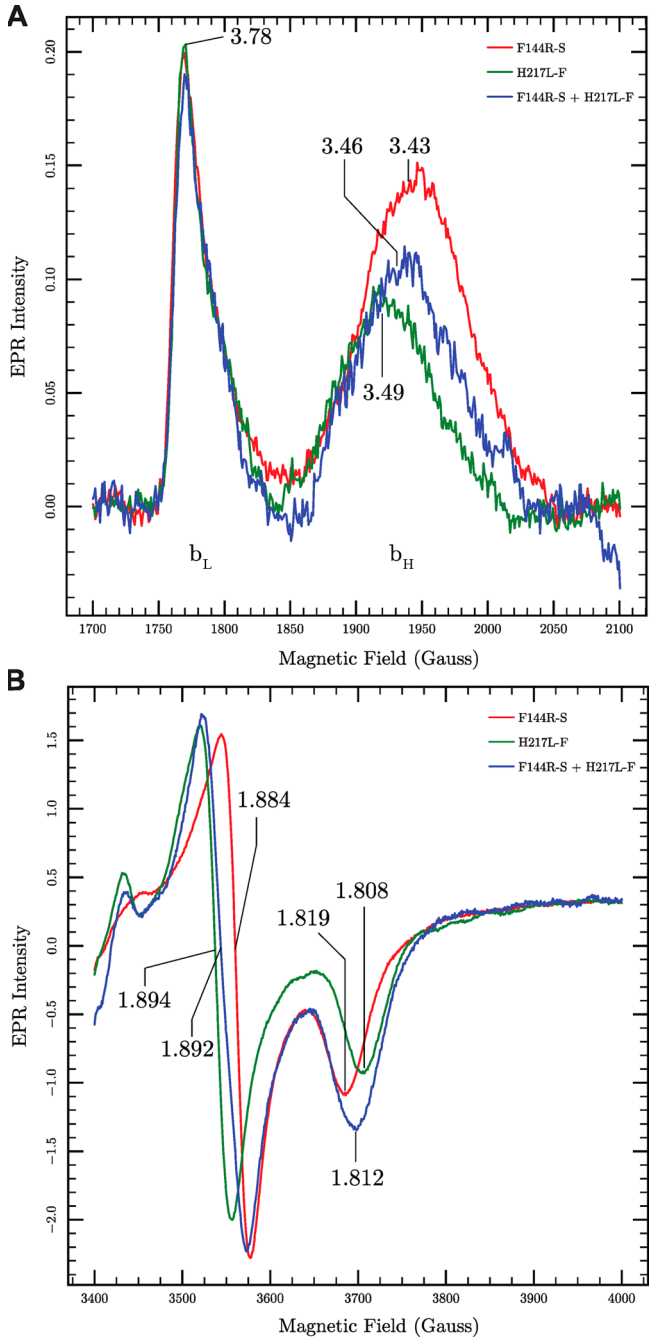

Figure 3. EPR characterization of *R. capsulatus* strains producing heterodimeric cytochrome bc_1 variants. (A) Low-spin heme EPR spectra of chromatophore membranes obtained from appropriate *R. capsulatus* strains grown by respiration in enriched medium. Spectra were recorded using partially oxidized (air-exposed, as-prepared) membranes derived from cells expressing cyt *b*-S F144R, cyt *b*-F H217L, and (cyt *b*-S F144R + cyt *b*-F H217L) cytochrome bc_1 variants. The following experimental conditions were used: temperature, 10 K; microwave power, 10 mW at 9.420 GHz; modulation amplitude, 10 G at 100 kHz, four scans. (B) [2Fe-2S] EPR spectra of ascorbate-reduced chromatophore membranes obtained from *R. capsulatus* strains listed in panel A and grown by respiration in enriched medium. The following experimental conditions were used: temperature, 20 K; microwave power, 2 mW at 9.416 GHz; modulation amplitude, 20 G at 100 kHz; one scan.

dx.doi.org/10.1021/bi400561e | *Biochemistry* 2013, 52, 7196−7206

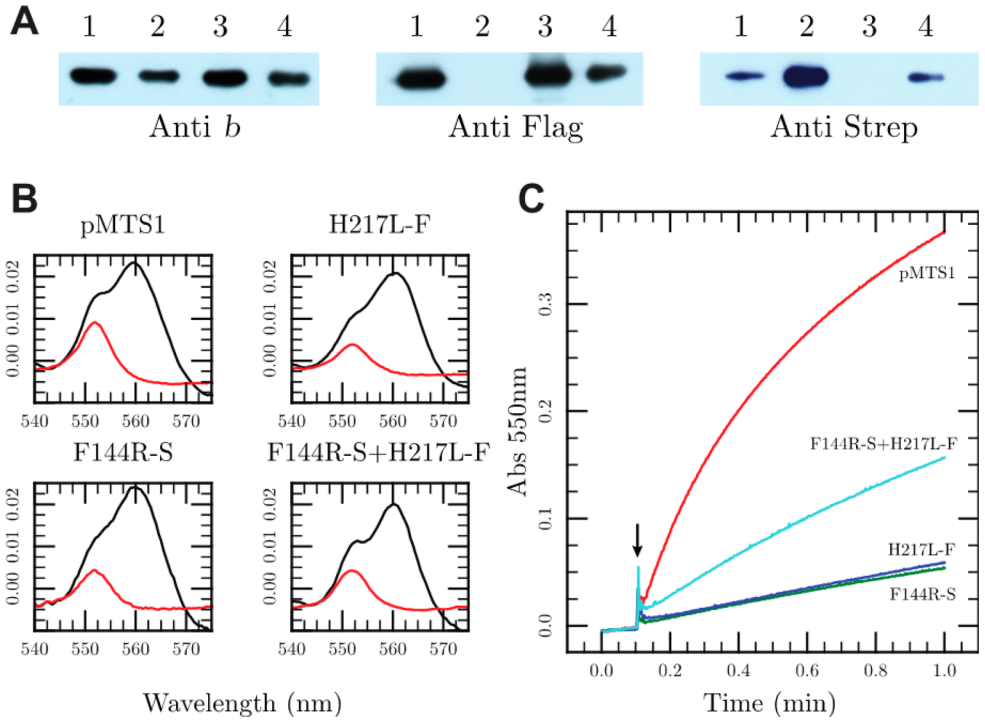

Figure 4. Biochemical properties of purified *R. capsulatus* homo- and heterodimeric cytochrome bc_1 variants. The homodimeric cyt *b*-S F144R and cyt *b*-F H217L (F144R-S and H217L-F, respectively) and heterodimeric (cyt *b*-S F144R + cyt *b*-F H217L) (F144R-S + H217L-F) cytochrome bc_1 variants were partially purified from cells harboring the two-plasmid system carrying the indicated cytochrome *b* mutations by DEAE-BioGel chromatography and then applied to two consecutive affinity chromatography steps (Strep followed by Flag binding columns) to fractionate the homodimeric and heterodimeric cytochrome bc_1 variants. (A) Purified samples were subjected to SDS−PAGE and immunoblot analyses using 10 μg of protein samples per lane, and the cytochrome *b* subunits were visualized using *R. capsulatus* specific polyclonal antibodies, as well as commercially available anti-Strep II or anti-Flag M2 monoclonal antibodies: lane 1, partially DEAE-BioGel purified cyt bc_1 containing both homo- and heterodimeric variants; lane 2, affinity-purified homodimeric cytochrome bc_1 variants tagged with the Strep epitope; lane 3, affinity-purified homodimeric cytochrome bc_1 variants tagged with the Flag epitope; lane 4, affinity-purified heterodimeric cytochrome bc_1 variants tagged both with Strep and Flag epitopes. (B) Optical redox difference spectra of the purified samples used in panel A together with a wild-type enzyme (pMTS1) to visualize their total *b*-type (dithionite-reduced minus ferricyanide-oxidized, black lines) and *c*-type (ascorbate-reduced minus ferricyanide-oxidized, red lines) cytochrome contents. (C) Steady-state cytochrome bc_1 activity of purified samples used in panel A together with a wild-type enzyme (pMTS1), measured by monitoring DBH_2:cytochrome *c* reduction at 550 nm on purified materials as described in Materials and Methods and the text.

2S] cluster g_y transition amplitudes were highly similar in different strains, indicating that the Fe−S protein was present in comparable amounts in all cases (Figure 3B). As expected, the shape and g_x values of the Fe−S protein [2Fe-2S] cluster signals were not identical in all mutants. Chromatophore membranes from cells producing the homodimeric cyt *b*-S F144R variant displayed a significantly narrowed and distorted [2Fe-2S] EPR spectrum, characterized by g_x = 1.819 and g_y = 1.884 features.[34] In contrast, the homodimeric cyt *b*-F H217L variant exhibited g_x = 1.808 and g_y = 1.894 features, which were identical to those seen with a wild-type cytochrome bc_1. Remarkably, membranes containing the heterodimeric (cyt *b*-S F144R + cyt *b*-F H217L) variant showed an intermediate EPR spectrum with characteristics associated with both cytochrome *b* mutations it carried. The [2Fe-2S] EPR spectrum displayed a slightly larger g_y resonance line at 1.892 and a larger g_x resonance line at 1.812 (Figure 3B). Overall, the EPR data established that these strains produced the expected mutant cytochrome bc_1 variants in comparable amounts.

Purification and Characterization of Epitope-Tagged Cytochrome bc_1 Variants. A two-step purification method, starting with anionic exchange (DEAE-BioGel), followed by epitope tag affinity chromatography, yielded large amounts of purified, mono-epitope-tagged homodimeric cyt *b*-S F144R and cyt *b*-F H217L, as well as double-epitope-tagged heterodimeric cytochrome bc_1 variants. SDS−PAGE and immunoblot analyses using specific cytochrome *b* and epitope tag antibodies (Figure 4A) and appropriate optical difference spectra (Figure 4B) established that the properties of purified, epitope-tagged homodimeric cytochrome bc_1 variants were comparable to those of their membrane-embedded versions. Next, a double-epitope-tagged heterodimeric cytochrome bc_1 produced by cells harboring the (cyt *b*-S F144R + cyt *b*-F H217L) mutations was purified as described in ref 19. DEAE-BioGel chromatography yielded partially purified and active [~0.6 μmol of cytochrome *c* min^{-1} (mg of total protein)$^{-1}$] cytochrome bc_1. These preparations were expected to contain two homodimeric (cyt *b*-S F144R and cyt *b*-F H217L) cytochrome bc_1 variants and one heterodimeric (cyt *b*-S F144R + cyt *b*-F H217L) cytochrome bc_1 variant (Figure 4A,B). Two consecutive affinity chromatography steps (Flag followed by Strep binding columns, and Strep followed by Flag binding columns) were used to separate the homodimeric and heterodimeric variants. When affinity chromatography was initiated with a Strep binding column, flow-through and subsequent wash fractions contained only Flag-tagged materials, which were attributed to the homodimeric cyt *b*-F H217L variant (Figure 4A, lane 2). Elution fractions contained both Strep- and Flag-tagged

dx.doi.org/10.1021/bi400561e | *Biochemistry* 2013, 52, 7196−7206

Table 1. Mass Spectrometry Analyses of Purified Cytochrome bc_1 Enzymes[a]

purified cytochrome bc_1	protease or treatment	cytochrome *b* peptide	peptide unique to
native homodimer (no tag control)	CNBr cleavage	M.VIYLLM*M*GTA**F**M@.G	F144 (wild type)
	chymotrypsin/aqueous	W.AF**H**TTGNNNPTGVEVR.R	H217 (wild type)
native-S homodimer (tag control)	chymotrypsin/60% methanol	F.NSHYGNPAE**W.S**	Strep tag
H217L-F homodimer (control)	CNBr cleavage	M.VIYLLM*M*GTA**F**M@.G	F144 (wild type)
	chymotrypsin/aqueous	**L**.TTGNNNPTGVEVR.R	H217L (mutant)
F144R-S homodimer (control)	CNBr cleavage	M.VIYLLM*M*GTA**R**M@.G	F144R (mutant)
F144R-S + H217L-F heterodimer	chymotrypsin/60% methanol	Y.GNPAE**WSHPQFEK.**	Strep tag
		A.SIEEDFNSHYGNPAE**DYKDDDDK**.-	Flag tag
	chymotrypsin/aqueous	W.AF**H**TTGNNNPTGVEVR.R	H217 (wild type)
		F.**L**TTGNNNPTGVEVR.R	H217L (mutant)
	CNBr cleavage	M.VIYLLM*M*GTA**F**M@.G	F144 (wild type)
		M.VIYLLM*M*GTA**R**M@.G	F144R (mutant)

[a]Purified homodimeric (cyt *b*-S F144R and cyt *b*-F H217L) and heterodimeric (cyt *b*-S F144R + cyt *b*-F H217L) cytochrome bc_1 variants were analyzed by nLC−MS/MS spectrometry as described in Materials and Methods. Amino acid modifications and corresponding mass changes are indicated as follows: methionine oxidation (*, +16), homoserine formation (@, −30), and homoserine lactone formation (#, −48). The MS/MS spectra of the peptides listed are provided in Table S1 of the Supporting Information, together with a larger and redundant list of relevant peptides detected in these analyses.

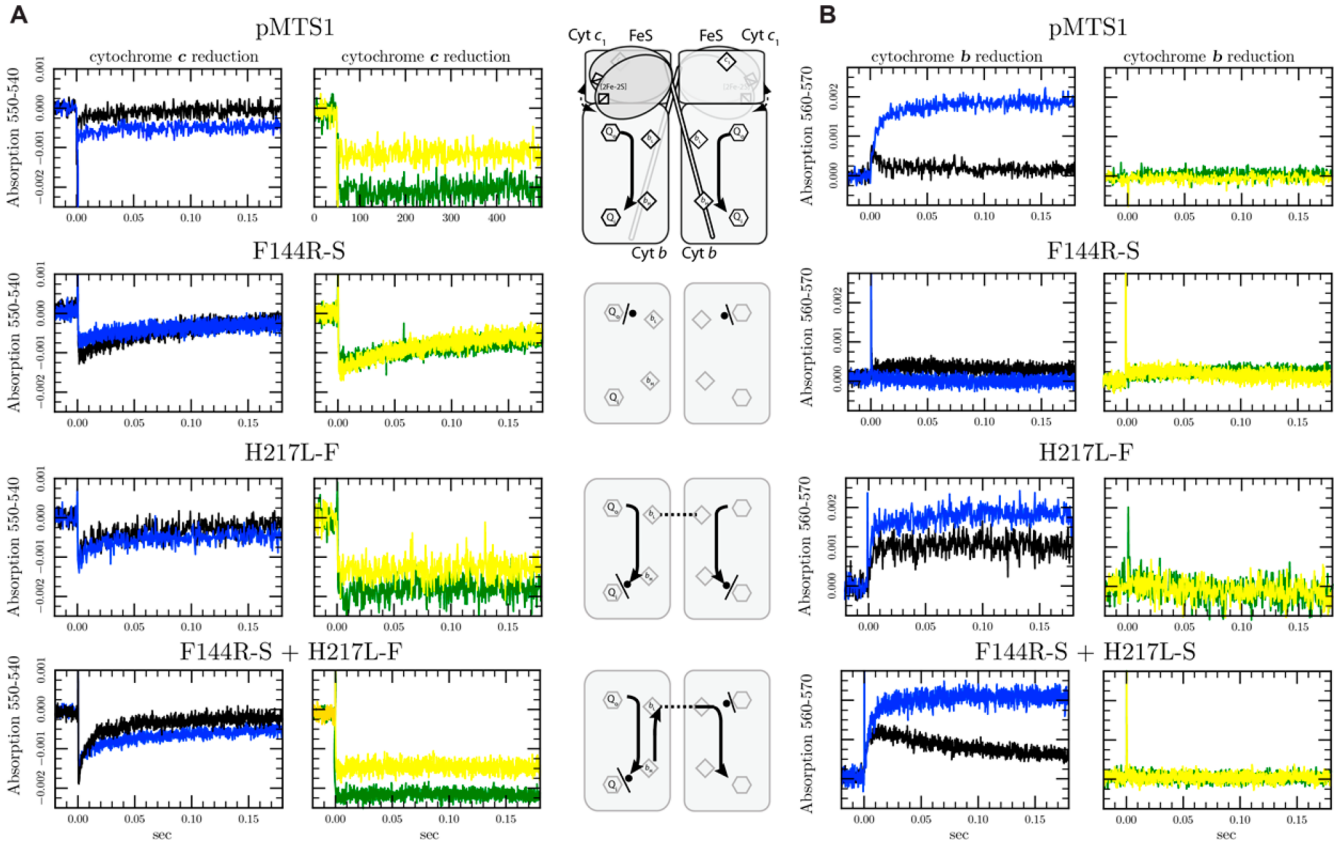

Figure 5. Light-induced, time-resolved cytochrome *b* reduction and cytochrome *c* re-reduction kinetics of various *R. capsulatus* strains. *R. capsulatus* strains producing wild-type (pMTS1), homodimeric cyt *b*-S F144R (F144R-S), homodimeric cyt *b*-F H217L (H217L-F), and heterodimeric (cyt *b*-S F144R + cyt *b*-F H217L) (F144R-S + H217L-F) cytochrome bc_1 variants were analyzed. In all cases, chromatophore membranes corresponding to an amount of reaction center equal to 0.30 μM were resuspended in 50 mM MOPS buffer (pH 7.0) containing 100 mM KCl poised at an ambient redox potential (E_h) of 100 mV. (A) The cytochrome *c* re-reduction kinetics were monitored at 550 nm minus 540 nm, in the absence of inhibitor (black), in the presence of 10 μM Q_i site inhibitor antimycin (blue), or in the presence of 10 μM myxothiazol (yellow), which abolishes QH_2 oxidation at the Q_o site, or 10 μM famoxadone (green), which abolishes the transfer of an electron from the [2Fe-2S] cluster to heme c_1 by immobilizing the head domain of the Fe−S protein at the Q_o site: first row, wild-type pMTS1; second row, homodimeric cyt *b*-S F144R; third row, homodimeric cyt *b*-F H217L; fourth row, heterodimeric (F144R-S + H217L-F) cytochrome bc_1 variants. (B) The cytochrome *b* reduction kinetics were monitored at 560 nm minus 570 nm, in the absence of inhibitor (black), in the presence of 10 μM Q_i site inhibitor antimycin (blue), in the presence of 10 μM myxothiazol (yellow), or in the presence of 10 μM famoxadone (green). In each case, the electron transfer events attributed to the kinetic traces are indicated by black arrows using a dimeric cytochrome bc_1 represented schematically in the central panel between panels A and B.

dx.doi.org/10.1021/bi400561e | *Biochemistry* 2013, 52, 7196−7206

material, attributed to the homodimeric cyt *b*-S F144R and the heterodimeric (cyt *b*-S F144R + cyt *b*-F H217L) variants. These fractions were concentrated by ultrafiltration, loaded onto a Flag binding column, and washed to remove the homodimeric cyt *b*-S F144R variants (Figure 4A, lane 3). Subsequent elution from this column yielded the heterodimeric (cyt *b*-S F144R + cyt *b*-F H217L) cytochrome bc_1 (Figure 4A, lane 4). Purified wild-type cytochrome bc_1 had a turnover activity of ~57−64 s^{-1} (micromoles of cytochrome *c* reduced per second per micromole of cytochrome *b*). In contrast, purified mutant homodimeric cyt *b*-S F144R and cyt *b*-F H217L variants had ~20-fold lower turnover activities of ~2.6−3.8 s^{-1} (Figure 4C). The purified heterodimeric enzyme was active with a turnover activity of ~15 s^{-1}, corresponding to ~25% of the turnover activity of a purified wild-type cytochrome bc_1 (Figure 4C).

Physical Evidence of the Production of a Heterodimeric *R. capsulatus* Cytochrome bc_1. Purified heterodimeric (cyt *b*-S F144R + cyt *b*-F H217L) cytochrome bc_1 variants were analyzed by liquid chromatography and tandem mass spectrometry (nLC−MS/MS) to physically document the presence of both wild-type and mutant forms of epitope-tagged cytochrome *b*, as expected with a heterodimeric, asymmetrical cytochrome bc_1 (Figure 1). Special care was applied to optimize the digestion conditions and mass spectrometry parameters to detect the peptides encompassing positions 144 and 217 and the carboxyl terminus of cytochrome *b* (Materials and Methods), and these peptides are listed in Table 1. An exhaustive list of all peptides detected at similar levels using wild-type homodimeric cyt *b*-S F144R and cyt *b*-F H217L as well as mutant heterodimeric (cyt *b*-S F144R + cyt *b*-F H217L) cytochrome bc_1 samples and the related spectra are included in the Supporting Information (Table S1).

Homodimeric wild-type cytochrome bc_1 samples contained only the wild-type [M.VIYLLMMGTA$\underline{F}_{144}$M.G] and [W.AF$\underline{H}_{217}$TTGNNNPTGVEVR.R] peptides, which encompass positions 144 and 217 of cytochrome *b*, respectively. Similarly, homodimeric mutant cytochrome bc_1 samples contained only the [Y.LLMMGTA$\underline{R}_{144}$MGY.L] or [F.$\underline{L}_{217}$TTGNNNPTGVEVR.R] peptide in the case of cyt *b*-S F144R or cyt *b*-F H217L, respectively, with the Phe to Arg substitution at position 144 or His to Leu substitution at position 217 of cytochrome *b*. On the other hand, the heterodimeric cytochrome bc_1 samples yielded all peptides detected with both wild-type and homodimeric mutant samples (Table 1). In addition, analyses of the C-terminal peptides of cytochrome *b* revealed the presence of only the Strep [Y.GNPAEWSHPQ$\underline{\text{FEK}}$] or Flag [A.SIEEDFNSHYGNPAE$\underline{\text{DYKDDDDK}}$] (underlined) tag in the case of the homodimeric samples, whereas both of these tags were detected with purified heterodimeric cytochrome bc_1, further confirming the SDS−PAGE and immunoblot data (Figure 4A). Overall, data indicated that the purified heterodimeric double-epitope-tagged and active cytochrome bc_1 variants had the cyt *b* F144R and cyt *b* H127L mutations, their native counterparts, and their associated epitope tags as expected.

Light-Activated, Single-Turnover Cytochrome *c* and Cytochrome *b* Reduction Kinetics of Homodimeric and Heterodimeric Cytochrome bc_1 Variants. The cytochrome *c* re-reduction and cytochrome *b* reduction kinetics were monitored as described previously[19] by light-activated, time-resolved optical kinetic spectroscopy using chromatophore membranes derived from appropriate cells harboring cytochrome bc_1 variants in RecA$^+$ (Figure 5) and RecA$^-$ (Figure S1 of the Supporting Information) backgrounds. Typical cytochrome *c* re-reduction kinetics were observed with wild-type membranes in the presence and absence of inhibitors (Figure 5A, top row). Membranes derived from cells producing the cyt *b*-S F144R homodimer exhibited very slow cytochrome *c* re-reduction either in the absence or in the presence of any inhibitor, in agreement with the presence of an inactive cytochrome bc_1 with two defective Q_o sites (Figure 5A, second row). Interestingly, in the presence of famoxadone (a stigmatelin-like Q_o site inhibitor), the full extent of cytochrome *c* oxidation was not seen in this mutant,[34] suggesting that its Q_o site might be highly refractory to this inhibitor. On the other hand, in chromatophore membranes from cells harboring the cyt *b*-F H217L homodimers, some cytochrome *c* re-reduction kinetics were detected (Figure 5A, third row). As described previously,[32] these kinetics were faster than those observed with cyt *b*-S F144R homodimers but slower than those with a wild-type cytochrome bc_1. Finally, cells producing the heterodimeric (cyt *b*-S F144R + cyt *b*-F H217L) variant exhibited cytochrome *c* re-reduction kinetics that were much faster than those seen with the cyt *b*-F H217L homodimer but slower than those observed with a wild-type strain (Figure 5A, bottom row). As expected, chromatophore membranes containing the homodimeric cyt *b*-F H217L or heterodimeric (cyt *b*-S F144R + cyt *b*-F H217L) variants showed cytochrome *c* re-reduction kinetics that were myxothiazol or famoxadone sensitive, unlike those with the cyt *b*-S F144R variant.

The cytochrome *b* kinetics exhibited by these strains in the absence or presence of antimycin were very interesting (Figure 5B). First, typical cytochrome *b* kinetics with a rapid reduction followed by a rapid oxidation were seen with wild-type membranes in the absence of inhibitor (Figure 5B, top row). In contrast, the cytochrome *b* reduction−oxidation reaction was not seen with membranes containing the homodimeric cyt *b*-S F144R mutant (Figure 5B, second row), as expected with a mutant lacking an active Q_o site.[34] In the case of the homodimeric cyt *b*-F H217L mutant, a partial cytochrome *b* reduction was observed in the absence of inhibitor (Figure 5, third row), reflecting an incomplete cytochrome *b* oxidation due to the absence of a stable Q/SQ at the Q_i site, as reported previously.[32] Remarkably, the chromatophore membranes containing the heterodimeric (cyt *b*-S F144R + cyt *b*-F H217L) variant exhibited cytochrome *b* kinetics with a slow transient oxidation readily observed on the time scale used (~50% oxidized after 150 ms vs the wild type, which is virtually 100% oxidized after 20 ms) (Figure 5B, bottom row). In this case, the initial rate of cytochrome *b* reduction was slower than that seen with a wild-type cytochrome bc_1, which exhibits a decay roughly complete after the reaction. Upon addition of antimycin A, which eliminates the transfer of an electron from heme b_H to the resident Q at the Q_i site, rapid and stable (on a time scale of 150 ms) cytochrome *b* reduction was seen with membranes derived from the wild type, the homodimeric cyt *b*-F H217L cytochrome bc_1 variant, and the heterodimeric (cyt *b*-S F144R + cyt *b*-F H217L) cytochrome bc_1 variant. As expected, these kinetics were not detected with the Q_o site defective cyt *b*-S F144R mutant. Moreover, in all cases, the cytochrome *b* reduction kinetics were sensitive to the Q_o inhibitors myxothiazol and famoxadone, confirming that the kinetics monitored indeed originated from Q_o site catalysis. Because both of the homodimeric variants are inactive with respect to the electron transfer processes examined, the slow

dx.doi.org/10.1021/bi400561e | *Biochemistry* 2013, 52, 7196−7206

reoxidation of cytochrome *b* reduction kinetics reflected the intrinsic properties of the heterodimeric (cyt *b*-F H217L + cyt *b*-S F144R) variant. The fast cytochrome *b* oxidation in a wild-type enzyme is generally attributed to the transfer of an electron from reduced cytochrome b_H to the Q_i site occupant Q or SQ (Figure 5, top row). Available data indicate that a major difference among the wild-type, homodimeric cyt *b*-F H217L, and heterodimeric (cyt *b*-S F144R + cyt *b*-F H217L) cytochrome bc_1 variants is their Q_i site Q/SQ occupancy.[32] We therefore attributed the slow cytochrome *b* reoxidation observed with the heterodimeric (cyt *b*-S F144R + cyt *b*-F H217L) cytochrome bc_1 variant to internal equilibration of electrons between all *b* hemes by "reverse" (i.e., among b_H, b_L, b_L, and b_H hemes) intermonomer electron transfer (Figure 5, bottom row). This slower electronic communication leading to the generation of SQ/QH_2 at the only active Q_i site of the heterodimeric enzyme provided sufficient turnover activity (~25% of that of the wild type) to sustain cyclic electron transport between the photochemical reaction center and cytochrome bc_1 to efficiently support Ps growth of *R. capsulatus*.

DISCUSSION

In this study, we characterized a new heterodimeric cytochrome bc_1 variant using a two-plasmid system similar to that described in detail in the preceding paper (DOI: 10.1021/bi400560p). First, given the small distances that separate the cytochrome *b* mutations used and their associated epitope tags, we found that these strains do not undergo detectable genetic rearrangements that might lead to the loss or segregation of the genetic markers used. Thus, even if such events occur, their products are beyond the limits of detection of the biochemical analyses pursued. The robustness of the two-plasmid system, combined with the precautions for avoiding selective growth conditions, and the use of shorter culture times established that the experimental data obtained are reliable.

Second, the new heterodimer carrying the (cyt *b*-S F144R + cyt *b*-F H217L) Q_o and Q_i site mutations had no effect on the structural stability of cytochrome bc_1. This enzyme contained all of its catalytic cofactors and was active under both *in vivo* and *in vitro* conditions. A strain carrying this new two-plasmid system supported the cytochrome bc_1-dependent Ps growth of *R. capsulatus* and showed interesting intermonomer electron transfer properties. Using the same cells, it was possible to conduct large-scale purification of homodimeric and heterodimeric cytochrome bc_1 variants, which exhibited ~5 and ~25% of wild-type cytochrome bc_1 turnover activity, respectively. Moreover, mass spectrometry analyses established that purified samples contained the cytochrome *b* mutations and their wild-type counterparts associated with appropriate epitope tags. Heterodimeric variants with linked cytochrome *b* subunits of cytochrome *b*-bc_1 enzymes have been reported previously.[18,35] Previously, no active *R. capsulatus* heterodimeric native cytochrome bc_1 could be purified because the previously available heterodimeric (cyt *b*-S Y147A + cyt *b*-F H212N) variant lost its activity during purification.[19] The new heterodimeric (cyt *b*-S F144R + cyt *b*-F H217L) cytochrome bc_1 variant readily overcame this limitation.

A remarkable finding of this study was the electron transfer properties observed with the new heterodimeric cytochrome bc_1, which lacks a stable Q_i site occupant (Q/SQ) in one of its monomers. Strains producing heterodimeric (cyt *b*-S F144R + cyt *b*-F H217L) cytochrome bc_1 variants exhibited unusual cytochrome *b* reduction and reoxidation kinetics at an ambient redox potential (E_h) of 100 mV, in the absence of inhibitors (Figure 5). Cytochrome *b* kinetics were clearly distinct from those usually seen with either a wild-type or a Q_i site defective homodimeric cyt *b*-F H217L cytochrome bc_1.[32] With the heterodimeric enzyme, a single flash of light triggered a cytochrome *b* reduction (observed at a time range of up to ~10 ms), which preceded a slow reoxidation phase that took more than 150 ms to reach completion. At the same E_h and in the absence of an inhibitor, wild-type cytochrome bc_1 also exhibits biphasic (often poorly resolved on the millisecond time scale) cytochrome *b* reduction kinetics. However, these kinetics are more than an order of magnitude faster and roughly complete within the ~5−10 ms time span. As expected, with the homodimeric cyt *b*-F H217L mutant that lacks a stable Q/SQ at both its Q_i sites,[32] in the absence of inhibitor at an E_h of 100 mV, a fast reduction but no reoxidation of cytochrome *b* was observed. The amplitude of this cytochrome *b* reduction corresponded roughly to one-half of that seen in the presence of antimycin and persisted for at least 150 ms. These observations support electron equilibration between hemes b_H and b_L of cytochrome bc_1, but because the E_m values of these hemes are highly affected by addition of antimycin in the cyt *b*-F H217L mutant, rigorous interpretation of the data remains difficult.[32]

In the presence of antimycin, which eliminates the Q_i site residents (Q/SQ) and blocks rapid reoxidation of cytochrome *b* via the transfer of an electron from reduced heme b_H to Q/SQ, comparable cytochrome *b* reduction kinetics were observed with wild-type, homodimeric cyt *b*-F H217L, and heterodimeric (cyt *b*-S F144R + cyt *b*-F H217L) cytochrome bc_1 variants. The major difference among these cytochrome bc_1 variants is the number of Q/SQ occupied active Q_i sites (i.e., two for the wild type, one for the heterodimeric mutant, and none for the homodimeric mutant). We attributed the slow cytochrome *b* reoxidation kinetics seen only with the heterodimeric variant (Figure 5B) to the occurrence of electronic equilibration among all four *b* hemes, ultimately conveying electrons to the Q/SQ resident of the only active Q_i site of the enzyme. Provided that this interpretation is valid, reverse intermonomer electron transfer occurs to bridge the b_H, b_L, b_L, and b_H hemes to the active Q_i site present only on one of the two monomers. Qualitatively, the rate of this multistep electron transfer process, estimated by cytochrome *b* reoxidation rates, appears to be slower than intramonomer electron transfer that occurs from b_L and b_H hemes to the active Q_i on the same monomer (i.e., a wild-type enzyme) when possible, as seen by the cytochrome *b* reoxidation rates in the absence of an inhibitor and reduction rates in the presence of antimycin. These studies complemented the initial observations of direct intermonomer electron transfer that our group and others have reported.[17−19] The findings rationalize why the heterodimeric (cyt *b*-S F144R + cyt *b*-F H217L) cytochrome bc_1 variant has a slower turnover than a native enzyme and show that its catalytic efficiency is sufficient for physiological Ps growth of *R. capsulatus*.

Comparison of the intermonomer electron transfer events that are observed using the previously studied heterodimeric (cyt *b*-S Y147A + cyt *b*-F H212N) cytochrome bc_1 variant[19] with those of the (cyt *b*-S F144R + cyt *b*-F H217L) variant is informative. Both of these heterodimeric variants were produced using a two-plasmid system in identical backgrounds together with inactive homodimers, and they had one defective Q_o site (i.e., cyt *b* F144R and cyt *b* Y147A mutations) on one monomer and one defective Q_i site (i.e., cyt *b*: H212N and cyt

b H217L mutations) on the other monomer. However, the effects of these mutations on Q_o and Q_i site catalysis are different.[21,22,31,32] Given that experimentally observed cytochrome *b* kinetics reflect multiple distinct steps of electron transfer, rigorous comparisons and interpretations are difficult. Nonetheless, in the absence of any inhibitor, the cytochrome *b* reduction and reoxidation kinetics observed with a heterodimer that has only one heme b_H coupled to an active Q_i site (cyt *b*-S Y147A + cyt *b*-F H212N)[19] seem faster (i.e., not time-resolved) than those seen with the heterodimer (cyt *b*-S F144R + cyt *b*-F H217L) used here that has two b_H hemes, of which only one is coupled to an active Q_i site [i.e., time-resolved (Figure 5B, last row)]. In the presence of antimycin that inactivates all available Q_i sites, cytochrome *b* reduction kinetics seem faster with the latter heterodimer than the former, in agreement with the previously formulated thermodynamic considerations.[36] This comparison indicates that in the case of a noninhibited heterodimeric enzyme lacking heme b_H on one monomer, the intermonomer electron transfer rate appears to be faster than what can be resolved on the millisecond time scale.

Finally, we note that the findings of this study are consistent with the "heterodimeric Q cycle" model,[15] which postulates dismutation of the two SQ molecules formed at the Q_i sites to yield Q and QH_2 required to initiate a consecutive turnover of cyt bc_1. Interactions between the Q_o and Q_i sites within a given monomer and between the two monomers of cytochrome bc_1 have been documented previously.[22,37] Structural elements of cytochrome *b* such as formation of SQ at a Q_i site were proposed to act as a trigger for QH_2 oxidation at the cognate Q_o site with helix E and *ef* loop extension acting as a temporal "gate".[16] Mutants that perturb these structural elements, like the b_H heme ligands (i.e., cyt *b* H212N) or the Q_i site occupancy (i.e., cyt *b* H217D, R, or L), also affect communications across membranes in cytochrome bc_1[22] and its temporal gates. Consequently, heterodimeric variants engineered using these mutations to inactivate the Q_o and Q_i sites of a given monomer are expected to remain active, although at levels lower than that of the native enzyme, as indeed observed in ref 35.

In summary, this study provides strong evidence that the two-plasmid system appears to be a reliable genetic platform for producing inactive homodimeric and active heterodimeric cytochrome bc_1 variants with novel characteristics. Studies of asymmetric and yet active variants might uncover hidden properties of a dimeric cytochrome bc_1 and, eventually, provide an answer to whether the second QH_2 oxidation during the modified Q cycle mechanism occurs consecutively at the same Q_o site or at two different Q_o sites of two monomers. In addition, light-activated millisecond time scale kinetic spectroscopy using chromatophores, which so elegantly contributed to our understanding of the modified Q cycle mechanism for many years,[11] is now insufficient. A more complete understanding of how cytochrome bc_1 functions might be better achieved by studies of purified heterodimeric cytochrome bc_1 variants with microsecond time scale spectroscopy[38] and successful resolution of their three-dimensional structures.

■ ASSOCIATED CONTENT

Supporting Information

Comprehensive list of peptides relevant to cytochrome *b* positions F144 and H217, wild type, mutations, and related epitope tags detected by nLC−MS/MS analyses, and spectra of relevant peptides (Figure S1), and light-activated cytochrome *c* re-reduction and cytochrome *b* reduction kinetics obtained using membranes from a (cyt *b*-S F144R + cyt *b*-F H217L) heterodimer-producing RecA$^-$ strain (Figure S2). This material is available free of charge via the Internet at http://pubs.acs.org.

■ AUTHOR INFORMATION

Corresponding Author

*E-mail: fdaldal@sas.upenn.edu. Telephone: (215) 898-4394. Fax: (215) 898-8780.

Funding

This work was supported by National Institutes of Health Grant GM 38237 and the Division of Chemical Sciences, Geosciences and Biosciences, Office of Basic Energy Sciences of the U.S. Department of Energy, through Grant DE-FG02-91ER20052 to F.D.

Notes

The authors declare no competing financial interest.

■ ABBREVIATIONS

Q, quinone; QH_2, hydroquinone; Tet, tetracycline; Kan, kanamycin; Ps, photosynthesis; Res, respiration; DBH_2, decylbenzoquinone; S-, Strep epitope tag; F-, Flag epitope tag; EPR, electron paramagnetic resonance.

■ REFERENCES

(1) Berry, E. A., Guergova-Kuras, M., Huang, L. S., and Crofts, A. R. (2000) Structure and function of cytochrome *bc* complexes. *Annu. Rev. Biochem. 69*, 1005−1075.

(2) Mitchell, P. (1976) Possible molecular mechanisms of the protonmotive function of cytochrome systems. *J. Theor. Biol. 62*, 327−367.

(3) Trumpower, B. L. (1990) The protonmotive Q cycle. Energy transduction by coupling of proton translocation to electron transfer by the cytochrome bc_1 complex. *J. Biol. Chem. 265*, 11409−11412.

(4) Daldal, F., Davidson, E., and Cheng, S. (1987) Isolation of the structural genes for the Rieske Fe-S protein, cytochrome *b* and cytochrome c_1 all components of the ubiquinol:cytochrome c_2 oxidoreductase complex of *Rhodopseudomonas capsulata*. *J. Mol. Biol. 195*, 1−12.

(5) Atta-Asafo-Adjei, E., and Daldal, F. (1991) Size of the amino acid side chain at position 158 of cytochrome *b* is critical for an active cytochrome bc_1 complex and for photosynthetic growth of *Rhodobacter capsulatus*. *Proc. Natl. Acad. Sci. U.S.A. 88*, 492−496.

(6) Berry, E. A., Lee, D.-W., Huang, L.-S., and Daldal, F. (2008) Structural and Mutational Studies of the Cytochrome bc_1 Complex. In *The Purple Phototrophic Bacteria* (Hunters, C. N., Daldal, F., Thurnauer, M. C., and Beatty, J. T., Eds.) pp 425−450, Springer, Dordrecht, The Netherlands.

(7) Xia, D. (1997) Crystal structure of the cytochrome bc_1 complex from bovine heart mitochondria. *Science 277*, 60−66.

(8) Iwata, S., Lee, J., Okada, K., Lee, J., Iwata, M., Rasmussen, B., Link, T., Ramaswamy, S., and Jap, B. (1998) Complete structure of the 11-subunit bovine mitochondrial cytochrome bc_1 complex. *Science 281*, 64−71.

(9) Berry, E. A., Huang, L.-S., Saechao, L. K., Pon, N. G., Valkova-Valchanova, M., and Daldal, F. (2004) X-ray structure of *Rhodobacter capsulatus* cytochrome bc_1: Comparison with its mitochondrial and chloroplast counterparts. *Photosynth. Res. 81*, 251−275.

(10) Crofts, A. R., Meinhardt, S. W., Jones, K. R., and Snozzi, M. (1983) Theory of the quinone pool in the cyclic electron-transfer chain of *Rhodopseudomonas sphaeroides*: A modified Q-cycle mechanism. *Biochim. Biophys. Acta 723*, 202−218.

(11) Crofts, A. R. (2004) The Q-cycle: A personal perspective. *Photosynth. Res. 80*, 223−243.

(12) De Vries, S., Albracht, S. P., Berden, J. A., and Slater, E. C. (1982) The pathway of electrons through QH_2:cytochrome *c*

oxidoreductase studied by pre-steady-state kinetics. *Biochim. Biophys. Acta 681*, 41−53.
(13) Gopta, O. A., Feniouk, B. A., Junge, W., and Mulkidjanian, A. Y. (1998) The cytochrome bc_1 complex of *Rhodobacter capsulatus*: Ubiquinol oxidation in a dimeric Q-cycle? *FEBS Lett. 431*, 291−296.
(14) Trumpower, B. L. (2002) A concerted, alternating sites mechanism of ubiquinol oxidation by the dimeric cytochrome bc_1 complex. *Biochim. Biophys. Acta 1555*, 166−173.
(15) Cooley, J. W., Lee, D.-W., and Daldal, F. (2009) Across membrane communication between the Q_o and Q_i active sites of cytochrome bc_1. *Biochemistry 48*, 1888−1899.
(16) Cooley, J. W. (2010) A structural model for across membrane coupling between the Q_o and Q_i active sites of cytochrome bc_1. *Biochim. Biophys. Acta 1797*, 1842−1848.
(17) Castellani, M., Covian, R., Kleinschroth, T., Anderka, O., Ludwig, B., and Trumpower, B. L. (2010) Direct demonstration of half-of-the-sites reactivity in the dimeric cytochrome bc_1 complex: Enzyme with one inactive monomer is fully active but unable to activate the second ubiquinol oxidation site in response to ligand binding at the ubiquinone reduction site. *J. Biol. Chem. 285*, 502−510.
(18) Swierczek, M., Cieluch, E., Sarewicz, M., Borek, A., Moser, C. C., Dutton, P. L., and Osyczka, A. (2010) An electronic bus bar lies in the core of cytochrome bc_1. *Science 329*, 451−454.
(19) Lanciano, P., Lee, D.-W., Yang, H., Darrouzet, E., and Daldal, F. (2011) Intermonomer electron transfer between the low-potential *b* hemes of cytochrome bc_1. *Biochemistry 50*, 1651−1663.
(20) Khalfaoui-Hassani, B., Lanciano, P., Lee, D.-W., Darrouzet, E., and Daldal, F. (2011) Recent advances in cytochrome bc_1: Intermonomer electronic communication? *FEBS Lett. 586*, 617−621.
(21) Saribaş, A. S., Ding, H., Dutton, P. L., and Daldal, F. (1995) Tyrosine 147 of cytochrome *b* is required for efficient electron transfer at the ubihydroquinone oxidase site (Q_o) of the cytochrome bc_1 complex. *Biochemistry 34*, 16004−16012.
(22) Cooley, J. W., Ohnishi, T., and Daldal, F. (2005) Binding dynamics at the quinone reduction (Q_i) site influence the equilibrium interactions of the iron sulfur protein and hydroquinone oxidation (Q_o) site of the cytochrome bc_1 complex. *Biochemistry 44*, 10520−10532.
(23) Darrouzet, E., Valkova-Valchanova, M., and Daldal, F. (2002) The [2Fe-2S] cluster E_m as an indicator of the iron-sulfur subunit position in the ubihydroquinone oxidation site of the cytochrome bc_1 complex. *J. Biol. Chem. 277*, 3464−3470.
(24) Sambrook, J. (2001) *Molecular Cloning: A Laboratory Manual*, 3rd ed., Cold Spring Harbor Laboratory Press, Plainview, NY.
(25) Gray, K. A., Davidson, E., and Daldal, F. (1992) Mutagenesis of methionine-183 drastically affects the physicochemical properties of cytochrome c_1 of the bc_1 complex of *Rhodobacter capsulatus*. *Biochemistry 31*, 11864−11873.
(26) Smith, P. K., Krohn, R. I., Hermanson, G. T., Mallia, A. K., Gartner, F. H., Provenzano, M. D., Fujimoto, E. K., Goeke, N. M., Olson, B. J., and Klenk, D. C. (1985) Measurement of protein using bicinchoninic acid. *Anal. Biochem. 150*, 76−85.
(27) Laemmli, U. K. (1970) Cleavage of structural proteins during the assembly of the head of bacteriophage T4. *Nature 227*, 680−685.
(28) Valkova-Valchanova, M. B., Saribaş, A. S., Gibney, B. R., Dutton, P. L., and Daldal, F. (1998) Isolation and characterization of a two-subunit cytochrome *b*-c_1 subcomplex from *Rhodobacter capsulatus* and reconstitution of its ubihydroquinone oxidation (Q_o) site with purified Fe-S protein subunit. *Biochemistry 37*, 16242−16251.
(29) Simpson, R. (2003) *Proteins and Proteomics*, Cold Spring Harbor Laboratory Press, Plainview, NY.
(30) Onder, O., Turkarslan, S., Sun, D., and Daldal, F. (2008) Overproduction or absence of the periplasmic protease DegP severely compromises bacterial growth in the absence of the dithiol:disulfide oxidoreductase DsbA. *Mol. Cell. Proteomics 7*, 875−890.
(31) Ding, H., Daldal, F., and Dutton, P. L. (1995) Ion pair formation between basic residues at 144 of the Cyt *b* polypeptide and the ubiquinones at the Q_o site of the Cyt bc_1 complex. *Biochemistry 34*, 15997−16003.
(32) Gray, K. A., Dutton, P. L., and Daldal, F. (1994) Requirement of histidine 217 for ubiquinone reductase activity (Q_i site) in the cytochrome bc_1 complex. *Biochemistry 33*, 723−733.
(33) Darrouzet, E., and Daldal, F. (2003) Protein-protein interactions between cytochrome *b* and the Fe-S protein subunits during QH_2 oxidation and large-scale domain movement in the bc_1 complex. *Biochemistry 42*, 1499−1507.
(34) Ding, H., Moser, C. C., Robertson, D. E., Tokito, M. K., Daldal, F., and Dutton, P. L. (1995) Ubiquinone pair in the Q_o site central to the primary energy conversion reactions of cytochrome bc_1 complex. *Biochemistry 34*, 15979−15996.
(35) Czapla, M., Borek, A., Sarewicz, M., and Osyczka, A. (2012) Enzymatic activities of isolated cytochrome bc_1-like complexes containing fused cytochrome *b* subunits with asymmetrically inactivated segments of electron transfer chains. *Biochemistry 51*, 829−835.
(36) Osyczka, A., Moser, C. C., Daldal, F., and Dutton, P. L. (2004) Reversible redox energy coupling in electron transfer chains. *Nature 427*, 607−612.
(37) Covian, R., Zwicker, K., Rotsaert, F. A., and Trumpower, B. L. (2007) Asymmetric and redox-specific binding of quinone and quinol at center N of the dimeric yeast cytochrome bc_1 complex. Consequences for semiquinone stabilization. *J. Biol. Chem. 282*, 24198−24208.
(38) Havens, J., Castellani, M., Kleinschroth, T., Ludwig, B., Durham, B., and Millett, F. (2011) Photoinitiated electron transfer within the *Paracoccus denitrificans* cytochrome bc_1 complex: Mobility of the iron−sulfur protein is modulated by the occupant of the Q_o site. *Biochemistry 50*, 10462−10472.